DOI 10.5162/ETTC2024/B2.2

A Review of FFT Algorithms and A Real-Time Algorithm Development for Airborne Vibration Testing Applications

Osman Birkan Ozseven[1, 2], Safak Tambova[3], Mustafa Helvaci[2]
[1] Department of Avionics and Electrical Systems, Turkish Aerospace, Istanbul 34467, Turkey; osmanbirkan.ozseven@tai.com.tr; +903128111800
[2] Department of Communication Systems, Istanbul Technical University, Istanbul 34467, Turkey; ozseven20@itu.edu.tr (O.B.O.); helvacim@itu.edu.tr (M.H.); +902123657800
[3] Department of Flight Test Systems, eRC-System GmbH, Ottobrunn 85521, Germany; tambova@erc-system.com; +4915110652823

Abstract

In Flight Test Instrumentation applications, many types of data are collected, including temperature, pressure, force, digital bus monitoring, etc. However, one type of data has always been popular and has become even more so with the increased use of composite structures: vibration. Vibration is a key measurement for different types of tests such as engine and propulsion system, flutter analysis, structural resonances, etc. In full-size air vehicle prototype testing, thousands or even ten thousand parameters are needed to be transformed over telemetry to the ground station. This operation itself already requires a significant amount of bandwidth in the communication channel and by considering the high-frequency behavior of vibration parameters, this situation becomes even worse. To overcome this problem, some techniques can be performed to increase the efficiency of communication by reducing the payload on the communication stream. The Fourier Transform decomposes a continuous-time signal into its foundational sinusoidal frequencies, bridging between the time and frequency domains. It reveals a signal's spectrum, denoting each frequency's strength and phase. This transformation is pivotal for understanding and isolating specific frequency components in continuous signals. The Discrete Fourier Transform (DFT) adapts the Fourier analysis to discrete-time signals, mapping a finite set of samples to a discrete frequency spectrum. It delineates the amplitudes and phases of sinusoids at distinct frequencies within digital signals. Central to digital signal processing, the DFT's efficiency is notably harnessed via the Fast Fourier Transform (FFT) algorithms. While conventional FFT algorithms are commonly favored, this paper distinguishes itself by adopting an alternative well-established method to achieve a more precise analysis in the real-time vibration analysis. In this paper, a review has been conducted to evaluate and compare well-known FFT algorithms. As a result of this review, the most efficient method has been used to solve a real-life aviation problem. The details of the problem have been given in the case-study chapter.

Key words: Chirp-Z Transform, Fast Fourier Transform, Flight Test Instrumentation, Real-Time Data Acquisition, Signal Processing, Vibration Testing.

Introduction

In the aerospace industry, data collection from air vehicles is crucial during the development or modernization stages while performing testing activities. The data which is obtained via air vehicle parts provides information about the efficiency of the systems. Although integrated systems have some standards, it is critical to see the system integrability with others [1]. To validate, verify, and certify the air vehicle in accordance with relevant standards, it is critical to implement a flight test instrumentation system design. This design should include a data acquisition unit, network switch, and recorder, all smoothly integrated with the existing aircraft systems throughout the various stages of air vehicle development [2]. Since, there can be a requirement for the installation of additional equipment such as a sensor, transducer, and thermocouple to be able to collect temperature, vibration, strain, current, voltage, pressure, etc. data from the avionics or mechanical parts [3] [4]. In this paper, vibration data is analyzed in detail.

Vibration data collected from sensors contains information about the mechanical behavior of air vehicle components such as avionics, propulsion systems, control surfaces,

gearboxes, and airframe structures. In terms of safety and reliability, excessive vibration may be a reason for mechanical problems or component wear. By monitoring vibrations, aircraft operators can detect issues early, reducing the risk of in-flight failures, accidents, or the health of various components due to mechanical failures [5] [6]. Irregular vibrations can indicate problems such as imbalance, misalignment, fatigue, or damage to these components [7]. Additionally, in the matter of compliance, regulatory authorities generally require aircraft operators to monitor and report on various parameters, including vibration levels. Conformity with these regulations is crucial to ensure the airworthiness and safety of aircraft [8]. In connection with research and development, aircraft manufacturers and researchers may use the obtained vibration data to improve the performance of the aircraft design and material. This data aids in the development of more efficient and reliable aircraft [9].

Fourier Transform (FT) is a fundamental technique that breaks down continuous-time signals into their component sinusoidal frequencies. It connects the time domain (where signals vary over time) to the frequency domain (where signals are represented by their frequencies). In the time domain, signals are complex waveforms formed by overlapping waves, each with its frequency, phase, and amplitude [10]. FT transforms this into a frequency spectrum, showing the strengths and phases of each frequency in the original signal. This is useful for identifying dominant frequencies. For discrete signals in digital applications, DFT is used, which maps a sequence of numbers (discrete signal) to another sequence representing its discrete frequency components. This spectrum reveals amplitudes and phases of discrete frequencies that approximate the original signal when combined [11].

DFT algorithms enable the analysis of signals in the frequency domain. These algorithms are crucial tools for decomposing discrete-time signals into their underlying frequency components. The Cooley-Tukey Radix-2 FFT, a widely used DFT algorithm, excels at efficiently computing the DFT for data lengths that are powers of 2 [12]. Mixed-radix FFT extends this approach to handle data lengths that are not powers of 2 by employing mixed-radix stages. The Prime Factor FFT specializes in efficiently computing the DFT of data with prime factorization lengths. Furthermore, Bluestein's FFT, also known as the Chirp Z-Transform (CZT), is vital when working with signals of arbitrary lengths, as it transforms them into a format suitable for FFT computation [13]. In the theory section, these algorithms are compared, and the most appropriate method is chosen for addressing the problem under consideration.

In this paper, a practical aviation challenge related to the propulsion system test is addressed. Specifically, during the propulsion system test, the transmission of vibration data to the ground station leads to significant constraints due to communication channel limitations. In response to this challenge, transmitting the vibration signal in its frequency domain format has been preferred, rather than the time domain signal, to facilitate real-time testing [14]. It's worth noting that a subsequent time domain analysis is also conducted during the post-data processing phase for comprehensive evaluation and insights. This approach allows to efficiently address the complexity of real-time data transmission and subsequent analysis in the context of aviation testing. In contrast to the widespread preference for conventional FFT algorithms in [15] and [16], this paper stands out by opting for the CZT Method, a well-established alternative, to attain a more precise analysis. Since, in spectral analysis, the frequency resolution of the FFT is intrinsically tied to the length of the signal window. This means that the resolution is determined by dividing the sampling rate by the number of points in the FFT. While zero-padding is a technique often employed to interpolate between FFT bins, it doesn't increase the genuine frequency resolution. On the other hand, the CZT introduces a significant flexibility. It allows for computation of the DFT samples within a specific region of the z-plane, enabling users to define a starting frequency, an ending frequency, and the desired number of points or frequency resolution between them. This capability of the CZT is particularly beneficial when the focus is on a specific frequency range rather than the entire spectrum. Band-Selectable Fast Fourier Transform (Zoom FFT) also provides targeted frequency analysis [17]. However, while Zoom FFT focuses on a specific frequency range through down-sampling after mixing to baseband, the CZT calculates spectral values across any chosen frequency interval directly. CZT also succeeds in handling non-uniformly sampled data, making it suitable for scenarios where data points are irregularly spaced in time [18].

This paper is organized as follows, a brief introduction to the topic covered by the paper is given in Chapter I. A theoretical comparison is made between different FFT algorithms and the

terms spectral leakage, windowing techniques, zero-padding and oversampling are given in Chapter II. Case study including the subjection of the propulsion system vibration analysis, the methods and techniques used in the CZT algorithm are given in Chapter III. Result analysis is performed in chapter IV. Concluding remarks are stated in Chapter V as performing CZT analysis in real-time.

Theory

In vibration analysis, the vibration data obtained from sensors placed on system components, continuously or at regular intervals are analyzed to predict whether there is a fault or not. Vibration signals taken from different points contain complex waveforms due to various forces and factors. Therefore, determining faults by examining time-waveform graphs is very challenging. The signals obtained in the time domain from vibration sensors are transformed into the frequency domain methods using the Fourier transform [19]. The frequencies within the spectrum provide valuable insights into not only the type but also the source of the fault, aiding in fault diagnosis. Concurrently, the amplitudes associated with these frequencies serve as a clear representation of the damage's severity, allowing for an accurate assessment of its extent. Specific faults occur at certain frequencies, and if the fault is not rectified, the amplitude at that frequency continues to increase. Faults exhibit various symptoms such as increased vibration, temperature, noise, and excessive current until the system malfunctions [7] [20]. Condition monitoring-based maintenance is performed by measuring and evaluating these symptoms. In this way, the risk of economic loss, operation problems and re-work caused by component failure may be reduced.

The Fourier Transform is a mathematical technique used to analyze signals or functions in terms of their frequency components. It decomposes a signal from the time domain into the frequency domain, revealing the individual sinusoidal components that make up the signal [21].

The Continuous Fourier Transform (CFT) is defined by using (1) [22].

$$X(f) = \int_{-\infty}^{\infty} x(t) e^{-j2\pi ft} dt \tag{1}$$

$X(f)$ is the complex-valued representation of the signal $x(t)$ in the frequency domain.

$x(t)$ is the signal in the time domain.

f is the frequency (in Hertz).

j is the imaginary unit.

The Inverse Continuous Fourier Transform (ICFT) is defined by using (2) [21].

$$x(t) = \int_{-\infty}^{\infty} X(f) e^{j2\pi ft} df \tag{2}$$

The DFT holds a significant position in the examination, creation, and realization of algorithms and systems in discrete-time signal processing applications, including but not limited to linear filtering, correlation analysis, and spectrum analysis. Its remarkable significance can be primarily attributed to the presence of highly efficient algorithms for its computation. DFT is equivalent to the samples of the FT at equally spaced frequencies. As a result, computing an N-point DFT involves calculating N samples of the FT of N equally spaced frequencies (2πk/N for k = 0 to N-1) on the unit circle in the z-plane. The main purpose is to use efficient algorithms for computing the N-point DFT, and these algorithms are commonly known as FFT algorithms [22].

When performing the computation of the DFT as outlined in (3), there is an essential involvement of *N* complex multiplications and *N-1* complex additions for each X(k) value. Consequently, in the process of calculating N DFT values, the necessity arises for N^2 complex multiplications and *N(N-1)* complex additions. It's also worth noting that within each complex multiplication, there is an implicit utilization of four real multiplications and two real additions, whereas every complex addition is achieved with two real additions [23]. As a result, for large values of *N* (the length of the array), computing DFT directly requires a considerable amount of processing. As *N* increases, the number of operations grows rapidly, and the computation becomes unacceptably time-consuming.

The DFT is defined by using (3). [22].

$$X[k] = \sum_{n=0}^{N-1} x[n] e^{j2\pi kn/N} \tag{3}$$

Where:

$X[k]$ is the complex−valued representation of the signal $x[n]$ in the frequency domain.

$x[n]$ is the discrete signal in the time domain.

k is the discrete frequency index (0 to $N-1$).

N is the number of data points in the time domain signal.

The Inverse Discrete Fourier Transform (IDFT) is defined by using (4) [22].

$$x[n] = \frac{1}{N}\sum_{k=0}^{N-1} X[k]e^{j2\pi kn/N} \quad (4)$$

The number of applications of the DFT in digital signal processing and other domains increased significantly because of the method created by Cooley and Tukey in 1965 to reduce the computation effort related to the DFT. The previously mentioned method additionally established the foundation for the development of diverse algorithms, commonly referred to as the FFT [24]. They significantly decrease the quantity of operations required for the computation of the DFT, hence enhancing the feasibility of the procedure. The FFT is a very fast and cost-effective algorithm utilized for the computation of the DFT. It offers useful simplification and computational convenience [25].

Spectral leakage is observed when the FFT is applied to a signal that does not contain an exact integer number of cycles within the window utilized for the transformation. This causes the signal's energy, which is concentrated at a single frequency, to be distributed across multiple frequency divisions in the FFT output [26]. The issue of FFT spectral leakage arises when the discrete frequency bins of the FFT do not fully line up with the frequency components of a signal. In order words, spectral leakage is especially pronounced when the signal frequency is not an integer multiple of the frequency bin spacing (bin width), the signal duration is not an integer multiple of the sampling period and the signal is not properly windowed before applying the FFT. To address spectral leakage, it is common practice to employ windowing techniques. These involve multiplying the original signal by a window function that reduces the signal's amplitude towards the edges [27]. This effectively reduces the influence of signal values at the edges of the window, which contributes to spectral leakage. Common window functions include Hamming, Hanning (or Hann), Blackman, and more. These windows taper the signal towards the edges, reducing abrupt changes that contribute to spectral leakage [19]. No leakage, leakage, and windowed sine wave comparison is shown in Fig. 1.

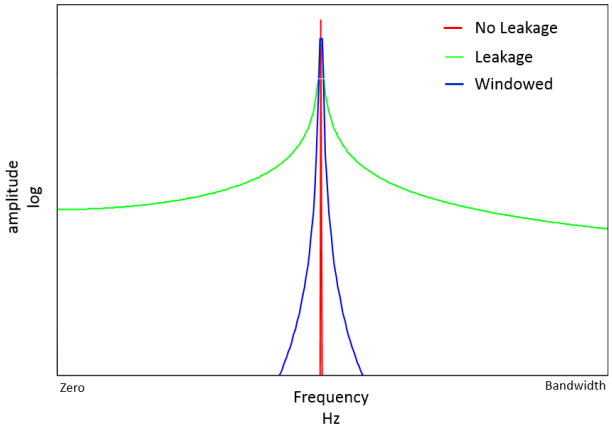

Fig.1. Sine wave: no leakage, leakage and windowed [28].

The Hamming window, whose formula is given in (5) has a main lobe that's wider than the main lobes of the Hanning and Blackman windows. It offers a good balance between main lobe width and side lobe suppression [29]. Also, it provides better side lobe suppression compared to rectangular (no window) but not as good as Hanning and Blackman.

$$w(n) = 0.54 - 0.46 * \cos\left(\frac{(2*\pi*n)}{N+1}\right) \quad (5)$$

Where:

$w(n)$ is the value of the Hamming window at the sample.

N is the total number of samples in the window.

n takes on integer values starting from 0 and goes up to N*-1.*

The Hanning window, which is mathematically defined in (6), is frequently known as the "raised cosine" window. The term "raised" or "shifted upwards" to initialize at 0 and conclude at 1 is derived from the geometric configuration of the function. The primary lobe of the window is thinner compared to the Hamming window, leading to greater frequency resolution. The amplitudes of the side lobes have a reduced magnitude in comparison to the Hamming function [27].

$$w(n) = 0.5 - 0.5 * \cos\left(\frac{(2 * \pi * n)}{N + 1}\right) \quad (6)$$

Where:

$w(n)$ is the value of the Hanning window at the sample.

N is the total number of samples in the window.

n takes on integer values starting from 0 and goes up to N*-1.*

The Blackman window, as defined in (7), has the narrowest primary lobe when compared to the other three windows. This feature offers optimal side lobe suppression, which means facilitating the reduction of spectral leakage [29]. Due to its strong side lobe suppression, the Blackman window can provide good results for precise frequency analysis.

$$w(n) = 0.42 - 0.5 * \cos\left(\frac{(2 * \pi * n)}{N-1}\right) + 0.08 * \cos\left(\frac{(4 * \pi * n)}{N-1}\right) \quad (7)$$

Where:

$w(n)$ is the value of the Blackman window at the sample.

N is the total number of samples in the window.

n takes on integer values starting from 0 and goes up to N-1.

All three windowing techniques (Hamming, Hanning, and Blackman) are designed to reduce spectral leakage when performing FFT analysis. The selection of the window to use is contingent on the demands and prerequisites. If frequency resolution and minimizing side lobes are concerned, Hanning or Blackman might be preferred. If a balance between frequency resolution and side lobe suppression is being looked for, Hamming could be a good choice [30]. Experimentation and understanding the signal characteristics help determine the best window for the application. There are some windowing techniques given in Table 1.

When working with vibration signals that contain high-frequency components, it is important to consider the specific characteristics of the signal and the requirements of the application. There are some other methods rather than the windowing method efficiently used while selecting a suitable FFT method such as zero padding, oversampling, etc.

In real-time FFT analysis, zero padding is commonly used to improve the accuracy and clarity of frequency analysis. It refers to the process of adding extra zeros to the end of a time-domain signal before performing the FFT [31]. The frequency resolution of FFT is determined by both the length of the input signal and the sampling rate (or the time duration of the signal). Longer signals provide finer frequency resolution, allowing you to distinguish between closely spaced frequencies more accurately. By adding zeros and increasing the signal length, the frequency resolution of the FFT is enhanced. Zero padding can also be seen as a form of interpolation between the existing signal samples. This can result in smoother spectral peaks in the frequency-domain representation, making it easier to visualize and analyse the frequency content of the signal [32]. Zero padding is often used in scenarios where frequency components with higher precision are aimed to be analysed, such as identifying closely spaced harmonics in a signal, or visualization of the frequency spectrum with more detail.

Tab. 1: Comparison of windowing techniques [23], [24], [25]

Signal Content	**Window**
Sine wave or combination of a mix of sinusoidal waves	Hann
Sine wave (with a focus on amplitude precision)	Flat Top
Narrowband stochastic signal (pertaining to vibration data)	Hann
Wideband stochastic signal (resembling white noise)	Uniform
Closely situated sinusoidal waves	Uniform, Hamming
Stimulus signals (akin to a hammer strike)	Force
Outcome signals	Exponential
Signals with undisclosed content	Hann
Two sinusoidal signals with proximate frequencies but distinct amplitudes	Kaiser - Bessel
Two sinusoidal signals with proximate frequencies and nearly identical amplitudes	Uniform
Precise measurement of amplitude in single-tone signals	Flat Top

Oversampling encompasses the act of obtaining and handling an increased number of samples from the vibration signal by utilizing a sampling rate that surpasses the Nyquist rate, equivalent to twice the maximum frequency component found within the signal. In mathematical terms, if the highest frequency component in the signal is f_{max}, then the Nyquist rate $f_{Nyquist}$ is given in (8) [33]. With more samples, better frequency resolution can be achieved. This means that closely spaced frequencies are distinguished more accurately, which can be beneficial in applications like

frequency analysis or spectral leakage reduction. Also, oversampling can help in reducing the impact of noise and quantization errors [34]. By capturing more samples, the noise gets spread over a wider range of samples, leading to a better signal-to-noise ratio (SNR) in the resulting FFT. The other advantage of oversampling is to reduce the effects of aliasing, which occurs when high-frequency components in the signal fold back into the frequency range of interest due to inadequate sampling. A higher sampling rate pushes the Nyquist frequency further away from the frequency range of interest, minimizing aliasing [35].

$$f_{Nyquist} = 2 \times f_{max} \quad (8)$$

There are several other methods and algorithms rather than FFT and DFT used for analysing and processing signals, especially in the field of signal processing and spectral analysis. Although the FFT and DFT are extensively utilized for the transformation of signals from the time domain to the frequency domain, it's important to note the existence of alternative methods like the Wavelet Transform (WT), Short-Time Fourier Transform (STFT), and Hilbert-Huang Transform (HHT). These alternative techniques are designed to address signal processing challenges and provide specific analytical requirements [36]. The WT is a mathematical method and signal processing tool employed to analyse signals and data in both the time and frequency domains. The utilization of this technique proves to be highly advantageous in the capture and analysis of high-frequency, non-stationary, and transient components within signals. The set of fundamental functions, commonly referred to as wavelets, are typically characterized by short durations and are defined at various scales [37]. Additionally, the STFT is a widely used technique in the field of signal processing that is utilized to analyse the changes in the frequency properties of a signal over time. The analysis of non-stationary signals, which exhibit time-varying frequency components, is significant [38]. Moreover, the HHT is a widely employed signal processing methodology utilized for the examination of non-linear and non-stationary data. The purpose of its development is to address the constraints inherent in conventional techniques such as the FFT and the STFT when dealing with intricate signals that change over time. The aim of this technique is to extract the inherent modes, uncover patterns, and analyse the instantaneous frequencies within signals [39]. FFT and DFT offer several advantages compared to other approaches and algorithms stated earlier. These advantages include improved efficiency and speed, enhanced frequency accuracy, wide applicability, compliance with linearity principles, and simplified implementation [40].

In the circumstance of high-frequency applications, it may be reasonable to explore higher-level algorithms that provide better performance or specific functionalities. An approach that can be utilized for high-resolution frequency analysis of signals with non-uniformly spaced frequency components is the Chirp Z-Transform (CZT) which is an extension of the DFT [41]. a contour adheres to the pattern as specified in (9).

$$z_k = AW^{-k} \quad (9)$$

Where:

k serves as the frequency index, spanning from 0 to $M-1$.

M is an arbitrary integer (not always equal to N, the point number of the desired complex spectrum).

A and W represent arbitrary complex numbers as defined in (10) [43].

$$A = A_0 e^{j\theta_0}, W = W_0 e^{j\varphi_0} \quad (10)$$

Where:

A is the contour starting point.

θ_0 is the starting angle.

W determines the rate at which the contour spirals inward or outward from a circle with a radius denoted as A_0.

φ_0 signifies the angular separation among the various frequencies.

When $A_0 = W_0 = 1$, $\theta_0 = 0$, $\varphi_0 = \frac{2\pi}{N}$ and $M = N$, the contour encompasses the full unit circle, and the CZT is essentially identical to the DFT.

Firstly, it is excellent at detecting transient events in the data due to its ability to provide high-resolution time-frequency information. FFT and DFT may be less effective in isolating and characterizing these events. Secondly, the CZT provides significant utility in the analysis of non-stationary signals or signals exhibiting time-varying frequency components and is better suited to capture these variations accurately [44]. In contrast, the FFT and DFT assume constant frequency content over the entire signal duration. Thirdly, if the signal contains chirping or rapidly changing frequencies, the CZT can track these changes in a way that FFT and DFT cannot. The CZT's chirp modulation

aligns with such frequency variations. Fourthly, the CZT can handle signals with arbitrary data lengths without requiring zero padding, making it versatile for various datasets [45]. FFT and DFT are most efficient when applied to data lengths that are powers of 2 [46].

The algorithm is used to compute the Z-transform of a sequence on a finely selected region of the Z-plane. When applied to vibration data analysis, especially in data acquisition (DAQ) systems the CZT can be beneficial in several ways such as focused frequency analysis, data compression, higher resolution, reduced noise, optimized data transmission and better feature extraction that can reduce the payload on a communication channel. In terms of focused frequency analysis, unlike the standard FFT that computes the spectrum uniformly across a wide frequency range, the CZT allows the user to focus on a specific frequency band of interest. This is especially useful when analysing vibration data where specific frequency bands are of interest [47]. Focusing on specific bands means fewer data points are needed, leading to less data to transmit. Regarding data compression, since only considering a particular frequency range, fewer data points are obtained than sending the entire frequency spectrum. By transmitting only the relevant frequency components, the amount of data can be reduced sent over a communication channel. Concerning higher resolution, using the CZT can yield higher resolution results within the specific frequency band of interest compared to a standard FFT applied to the same data. The CZT has the potential to identify anomalies or features that could go unnoticed when using alternative methods. In connection with reduced noise, in the case of focusing on a specific frequency band, irrelevant frequency components (which might be just noise or other undesired vibrations) can be excluded. This can result in a cleaner signal representation, requiring less data for effective transmission or storage. In the matter of optimized data transmission, in wireless DAQ systems, where bandwidth might be a constraint, sending only crucial or relevant information becomes a necessity. By utilizing CZT, it is essentially sending only the most pertinent information, thus optimizing the use of available bandwidth [41]. About better feature extraction, the CZT can help in extracting more meaningful features from vibration data by focusing on the relevant frequency components, which could be of a much smaller size than the original data, thus reducing the payload. Comparison of FFT, DFT and CZT is given in Table 2.

Tab. 2: Comparison of FFT, DFT and CZT [22], [23], [24]

Feature	FFT	DFT	CZT
Computational Efficiency	Highly efficient (O (N log N))	Standard (O(N^2))	Depends on the algorithm used
Time-Domain Input	Finite-length sequence	Finite-length sequence	Finite-length sequence
Frequency-Domain Output	Discrete frequencies	Discrete frequencies	Discrete frequencies
Frequency Resolution	Fixed based on signal length	Fixed based on signal length	Adjustable
Time-Frequency Analysis	Limited (non-time-localized)	Limited (non-time-localized)	Effective (time-localized)
Application Range	General spectral analysis	General spectral analysis	Time-varying signals
Real vs. Complex Output	Complex	Complex	Complex
Suitable for Linear Chirps	No	No	Yes
Computational Complexity	Lower for large N	Higher for large N	Depends on the algorithm used

Case Study

As detailed in Chapter I, vibration testing has remarkable importance in the aerospace industry, surrounding the assessment of aircraft components, systems, and even entire airframes to ensure their dependable and safe operation across diverse flight conditions. In this case study, the primary objective is to subject the prototype propulsion system to strict vibration analysis. After a detailed evaluation of available analysis methods, the decision has been made to employ the CZT technique to handle the challenges that appeared in the case study.

The exact frequency range of interest for vibration tests using the CZT depends on the specific goals of the test and the components being analyzed. The primary frequencies of interest here are associated with the engine's rotational speed and harmonics. This can vary from low frequencies like large turbofan engines to higher frequencies such as smaller engines or propellers. The CZT algorithm's ability to outline the specified frequency range with remarkable resolution enables effective "zooming in" on this specific range to identify

the engine harmonics relevant to the investigation [48].

Planned engine tests are set to run at 2000 RPM, meaning the engine completes 2000 rotations per minute, corresponding to a fundamental harmonic with a frequency determined by using (12) of 2000/60 = 33.33 Hz. This knowledge serves as a vital reference point for identifying the specific frequencies of interest during the frequency analysis. The choice of a frequency range spanning from 1 Hz to 512 Hz is planned, aimed at providing clear insight into the motor's harmonic behavior. Even when considering the 10th harmonic, the corresponding frequency value is calculated as 330 Hz using (11). Therefore, preferring a wide frequency range makes logical sense, as it ensures the capture of all potential frequency components, even if higher harmonics are not the primary focus.

$$f_{harmonic} = n \times f_{fundamental} \quad (11)$$

Where:

$f_{harmonic}$ is the harmonic frequency.

n is the harmonic number.

$f_{fundamental}$ is the fundamental frequency.

If the given parameters are substituted into (11),

$f_{harmonic} = 10 \times 33.33$

$f_{harmonic} = 330.33$

$f_{harmonic}$ is rounded to 330 Hz.

The provided algorithm (see Appendix A for the pseudocode) contains the methodology and computational steps for simulating real-time vibration data processing. Using the CZT, the provided algorithm emphasizes the specific frequency components, offering a detailed perspective on the signals in the frequency domain [49].

The given algorithm in the paper consists of vibration data extraction, defining key parameters, desired spectral resolution, pre-processing, CZT configuration, real-time processing simulation, visualization, playback, and performance assessment stages. In the data extraction stage, the algorithm loads vibration data from a TDMS (Technical Data Management Streaming) file. The acceleration values and corresponding time stamps are extracted from the data [50]. In the defining key parameters stage, key parameters are set, including the sampling frequency $f_s = 2048$ Hz denotes how frequently data is sampled, the $windowSize = 512$ samples defines the data segment length for spectral analysis, the $overlap = 256$ samples ensures smooth transitions between consecutive data segments and the $segmentSize = 512$ samples, which denotes the data chunk processed in one iteration.

In the iteration establishment stage, to process the vibration data in segments, the number of iterations (chunks) is determined by using (12).

$$Iterations = \frac{length\ of\ full\ data}{segments\ size} - 1 \quad (12)$$

Equation 12 ensures that each data chunk consists of non-overlapping segments, optimizing the computational efficiency.

In the spectral resolution and pre-processing stage, the vibration data is segmented into overlapping windows using the calculated parameters. Windowing helps reduce spectral leakage and improve frequency resolution. The process of oversampling with a 512-point Hann window and a sampling rate of 2048 Hz strengthens the resolution of frequency analysis [51]. The increased resolution facilitates an in-depth investigation of the frequency spectrum. It provides opportunities for advancements when necessary and enhances the precision with which high-frequency harmonics are detected, which allows for a greater understanding of the engine's behavior and performance.

The Hann window is utilized for the CZT analysis in this paper thanks to its numerous benefits. The selection of the Hann window is inspired by its ability to prevent spectral leakage, hence increasing the accuracy of frequency analysis [52]. It provides a consistent frequency response, facilitating the accurate identification of spectral peaks. Furthermore, this technique achieves a harmonious equilibrium between the width of the primary lobe and the suppression of side lobes, so increasing the resolution of frequencies while limiting the occurrence of unwanted sidelobe artefacts. Additionally, the Hann window is favored for its simplicity and ease of implementation, requiring minimal computational resources [53].

In a CZT, the desired resolution is computed by using (13) [54].

$$\text{The desired resolution} = f_s / windowSize \quad (13)$$

If the given parameters are substituted into (13),

$\text{The desired resolution} = 2048 / 512$

$\text{The desired resolution} = 4\ Hz$

This means that each bin in the frequency spectrum represents a 4 Hz bandwidth.

In the CZT configuration, each data segment's processing time is clocked. This provides invaluable insights into computational requirements. Data segments, produced with 512 samples and 256-sample overlap, ensure a consistent data flow. Unlike traditional Fourier Transforms, CZT allows focused spectral analysis in the range of 1 Hz to 512 Hz (as defined by f_{start} and f_{end}).

If M is defined as the number of points between f_{start} and f_{end} based on a desired frequency resolution, then M is computed by using (14). As mentioned in (10), M is not equal to N .

$$M = \frac{f_{end} - f_{start}}{desired\ resolution} + 1 \tag{14}$$

If the given parameters are substituted into (10),

$$M = \frac{512 - 1}{4} + 1$$

$$M = 128.75$$

M is rounded to 128 using the floor command.

The parameters α and ω for the CZT calculation are derived from (10) to apply (15) and (16). These parameters are essential for tuning the CZT to focus on the specified frequency range.

$$\alpha = e^{-1j \times 2\pi \times f_{start}/f_s} \tag{15}$$

$$\omega = e^{-1j \times 2\pi \times (f_{end} - f_{start})/(M \times f_s)} \tag{16}$$

Instead of producing a spectrum with 512 points (which would have been the case with a regular FFT of a 512-point signal), the CZT method produces a spectrum with only 128 points. This reduction is possible because CZT focuses only on the frequencies between f_{start} and f_{end}, with the defined resolution. In essence, for each segment of the data, this reduction enables to focus on the frequency components that are most relevant to the analysis, reduces the computational overhead by processing fewer data points and provides a more streamlined visualization that emphasizes dominant frequencies within the desired range while discarding information outside the desired frequency range.

In the real-time processing simulation, the main loop simulates real-time data acquisition and processing. For each iteration, the algorithm captures a data segment. CZT is applied to the windowed segment, producing a frequency spectrum for the desired range. The computed frequency domain data is stored for later visualization. In Acra KAM-500 modules, signals are sampled many times faster than specified by the user [55]. The KAD/ADC/111 is a dedicated hard-wired state machine which performs oversampling on all available channels at a rate within the range of 16,000 samples per second (16 ksps) to 32,000 samples per second (32 ksps). Additionally, the state machine incorporates digital filtering mechanisms to remove any noise components that exceed the user-defined cutoff frequency. This system ensures precise and efficient signal processing in the device. By using the information from [56], the average sample per second is calculated as 24 ksps. A simulated acquisition delay of 0.021 seconds is added to replicate the real-world acquisition timings by using (17).

$$Acquisition\ Delay = \frac{Segment\ Size}{Average\ ksps} \tag{17}$$

If the given parameters are substituted into (17),

$$Acquisition\ Delay = \frac{512}{24}$$

$$Acquisition\ Delay = 0.021\ seconds$$

In the visualization stage, the algorithm generates two plots: a time domain plot and a frequency domain plot. In the time domain plot, the vibration data is plotted against time, providing insights into the acceleration values over time. In the frequency domain plot, the CZT-derived frequency spectrum highlights the top 5 magnitudes to emphasize dominant frequencies [29]. A simulation ‘pause’ introduces a realistic feel during playback.

In the performance assessment, the processing time for each segment is recorded, and the average segment processing time is computed by using (18).

$$average\ time = \frac{1}{iterations} \sum T \tag{18}$$

Where:

T: Elapsed time for each iteration.

Using the CZT algorithm for propulsion system vibration analysis, despite its effectiveness and providing great solutions, presents challenges. These challenges include harmonic vibrations generated by rotating machinery, potential interactions with other propellers leading to instant frequencies, the presence of broadband noise unrelated to specific harmonics, and variations in vibration profiles across different operational states of the rotorcraft. To manage these, it's crucial to ensure sufficient resolution in frequency analysis, especially for distinguishing close frequencies when propeller

interactions are a concern. Additionally, having data from other propellers, even for reference, can be advantageous. Higher resolution analysis in spectral analysis requires more distinct frequency bins over a given range, enabling better discrimination between closely spaced frequency components [47].

Result Analysis

The real-time simulation has been performed using MATLAB® R2023a with the license number 41077201. The algorithm incorporates the following optimization techniques to enhance performance: memory pre-allocation, vectorization, and usage of built-in functions [57]. PARFOR library has been used to increase the real-time performance of the calculations.

Vibration data is collected using the PCB 33931 model vibration sensor [58]. This sensor is designed to capture vibrations in its surroundings and convert them into electrical signals. To ensure accurate data acquisition, the raw vibration signals are first subjected to signal conditioning. This process is facilitated by Curtiss-Wright hardware, which is specifically configured for various operations such as amplification, filtering, and noise reduction data acquisition to enhance the quality and relevance of the vibration data. The effectiveness of the algorithm hinges on its capacity to optimize computations across multiple CPU cores, resulting in a substantial reduction in processing time for handling large datasets [59]. The real-time CZT simulation has been run on a PC which has 12th Gen Intel Core, i7-12700H and 2.30 GHz.

In a complete evaluation containing all relevant factors, such as the CPU, hardware, and processor, the average time per iteration, which includes acquisition time, is calculated at 0.0315 seconds. This holistic analysis offers a broad perspective on the computational process, accounting for the diverse variables that affect performance. However, a more detailed examination, specifically concentrating on the CZT analysis, shows a remarkable change in efficiency. When isolating this aspect from the overall computation, the time per iteration dramatically reduces to 0.0017 seconds.

Time domain vibration signals and frequency domain CZT magnitude plots have been presented in Fig. 2, Fig. 3, and Fig. 4, showing the results of a real-time simulation executed through the methods detailed in Chapter III. These graphics are captured by taking screenshots at three randomly chosen points during the simulation. This approach provides a dynamic look into the evolving behavior of the system, offering valuable data that aids in the analysis and understanding of the simulated processes. The combination of time domain and CZT magnitude plots allows for a comprehensive examination of the system's response, making it an integral component of the case study in Chapter III.

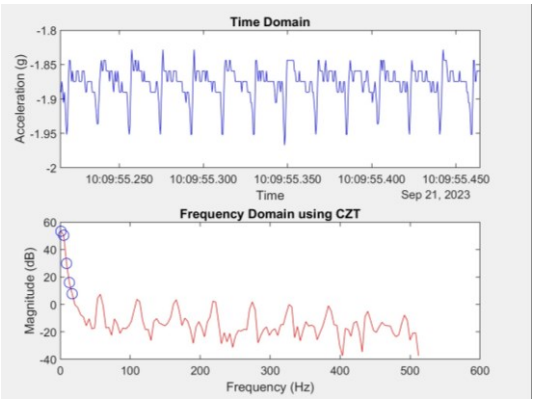

Fig.2. Time domain vibration signals and frequency domain Chirp Z Transform (CZT) magnitude plots.

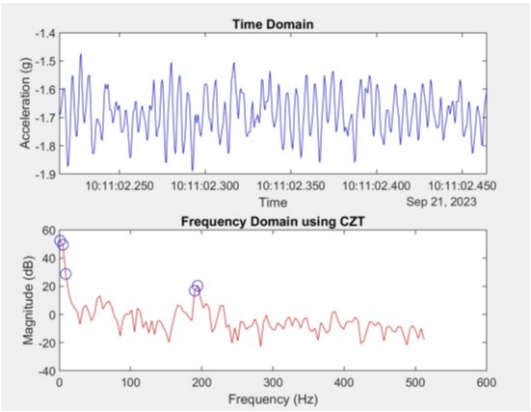

Fig.3. Time domain vibration signals and frequency domain Chirp Z Transform (CZT) magnitude plots.

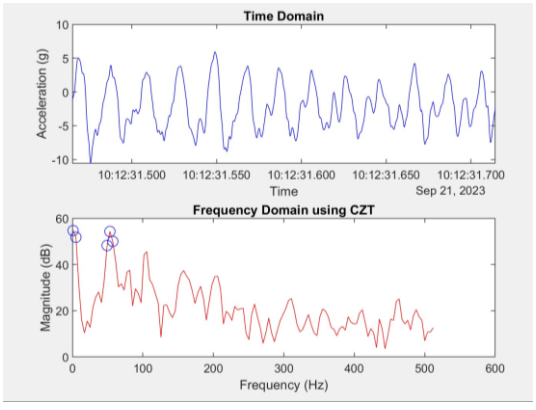

Fig.4. Time domain vibration signals and frequency domain Chirp Z Transform (CZT) magnitude plots.

Conclusion

Vibration data collected from sensors contains essential information about the mechanical behavior of structures and avionics, characterized by factors like frequency, amplitude, and phase. Time domain analysis reveals temporal behavior, while frequency domain analysis through CZT uncovers underlying frequency components. Real-time CZT analysis continuously processes incoming vibration data, finding applications in anomaly detection, pattern identification, and spectral analysis. This research seeks to enhance real-time data analysis, especially where high-frequency data is vital for decision-making. In the context of propulsion systems, vibration analysis is crucial for early issue detection, ensuring safety and efficiency [60].

This paper primarily focuses on optimizing high-frequency data payload using the CZT algorithm, regardless of sensor quality. The given methodology reduces the number of data points by a factor of 4 for each segment. To enhance the CZT algorithm, the Hann windowing technique is incorporated which minimizes spectral leakage, ensures a smooth frequency response, and is easy to implement [61]. In Chapter III, the CZT algorithm is applied to comprehensively analyze the prototype propulsion system. The process involves determining the desired spectral zoom range through harmonic calculation, leading to the definition of parameters like f_{start} and f_{end} As outlined in Chapter II, f_s is calculated using the oversampling method. After determining the f_s, the desired resolution is also calculated. These parameters play a crucial role in assigning CZT-specific coefficients, including M, α, and ω, significantly improving the precision and clarity of the engine harmonics analysis.

When existing similar studies are examined, it has been observed that FFT Algorithms are generally used in many real-time applications such as [12] and [16], and CZT is preferred for post-processing applications [62]. When the review results in Chapter II are evaluated, it is concluded that the best method for the case study given in Chapter III was a real-time CZT Algorithm. Additionally, this algorithm stands out among other CZT-based approaches by strategically utilizing pre-calculated exponential factors and a careful buffering scheme, which collectively ensure a computationally efficient execution without compromising the transformative precision. These attributes are particularly advantageous when dealing with high-volume or streaming vibration data in dynamic systems.

In summary, the CZT offers a focused and efficient way to analyze and represent vibration data, which can lead to substantial reductions in the amount of data that needs to be transmitted, especially when specific frequency bands are of interest. This results in a reduced payload on communication channels in DAQ systems.

In a forthcoming study, while real-time CZT analysis offers numerous benefits, it also leads to some challenges, such as its computational complexity for large datasets and optimized algorithms to handle data in real-time. Additionally, sensor quality, data transmission speed, and noise interference can affect the accuracy of results. To manage these challenges effectively, a custom CZT function may be developed. This custom function will handle specific research requirements, potentially enhancing accuracy and computational efficiency in the analysis.

Appendix

Appendix A - Pseudocode of the algorithm

start

read the vibration data from the TDMS file

set vibrationData to data{1, 1}.vibrationData

set time to data{1, 1}.Time2048Hz

set fs (sampling frequency) to 2048 Hz

set windowSize to 512

set overlap to 256

set segmentSize to 512

set f_start (start frequency) to 1

set f_end (end frequncy) to 512

create window = hann(windowSize)

calculate desired_resolution = fs / windowSize

calculate M = (f_end - f_start) / desired_resolution + 1

calculate a = exp(-1j * 2 * pi * f_start / fs)

calculate w = exp(-1j * 2 * pi * (f_end - f_start) / (M * fs))

compute iterations = floor(length(fullVibrationData) / segmentSize) – 1

for iteration from 1 to iterations

start a timer (tic)

calculate startIndex = (iteration - 1) * segmentSize + 1

calculate endIndex = iteration * segmentSize

calculatevibrationData=fullVibrationData(startIndex:endIndex)

calculate timeSegment = fullTime(startIndex:endIndex)

reshape the vibration data into overlapping segments using the 'buffer' function

compute the CZT of the reshaped data with the Hann window, M, w, and a

store the results, time segment, and original vibration data in a data structure

pause for 0.021 seconds (simulated processing time)

record and store the elapsed time for this iteration

end of loop

create a frequency vector 'frequencies' from f_start to f_end with M points

initialize an array 'top5Handles' to store handles for the top 5 plotted points

create a figure with two subplots for time and frequency domains

for iteration from 1 to iterations

update the time domain plot with current time and vibration data

calculate the magnitude of the CZT in decibels

if 'top5Handles' is not empty, clear the previous top 5 points

find the top 5 indices with the highest magnitude

extract the corresponding frequencies and magnitudes

plot the top 5 points on the frequency domain subplot

pause for 0.25 seconds for visualization

end of loop

calculate the average processing time per segment

display the average processing time

end

Acknowledgement

Here, sincere gratitude to the eRC Systems GmbH and Turkish Aerospace for their invaluable contributions to advancing research and scientific endeavors, providing researchers with a robust platform for innovation and discovery.

References

[1] O. B. Ozseven, S. Tambova and H. Helvaci, "A Risk Analysis Study: Model Development for Risk Mitigation and Systematic Approach to FTI System Design Activities," *2022 IEEE International Symposium on Systems Engineering (ISSE),* Vienna, Austria, 2022, pp. 1-6, doi: 10.1109/ISSE54508.2022.10005323.

[2] S. A. Kilpatrick and T. A. Newton, "The Unique Challenges of Testing Specialized Network-Based Data Acquisition Systems," *2014 IEEE AUTOTEST*, St. Louis, MO, USA, 2014, pp. 233-238, doi: 10.1109/AUTEST.2014.6935151.

[3] Ş. Tambova, and A. Aybar, "Colored Petri Nets Model for Network Based FTI Systems", *Journal of Communications,* vol. 16, no. 9, pp. 400-405, September 2021, doi: 10.12720/jcm.16.9.400-405.

[4] NASA SP-6105, Systems Engineering Handbook, Revision 2, 2016.

[5] T.D. Scharton, Force Limited Vibration Testing Monograph, NASA Reference Publication RP-1403, 1997.

[6] M. Mosher, A.H. Pryor and D. G. Lewicki, "Detailed Vibration Analysis of Pinion Gear with Time-Frequency Methods," NASA, 2003.

[7] P. K. Aggarwal, "Dynamic (Vibration) Testing: Design Certification of Aerospace System." Encyclopedia of Aerospace Engineering, 2010.

[8] A. Halfpenny and T. C. Walton, "New Techniques for Vibration Qualification of Vibrating Equipment on Aircraft", *Aircraft Airworthiness & Sustainment 2010,* 2010.

[9] Crounse, David R., "Flight Test Instrumentation", AGARD Flight Test instrumentation Series, AGAR Dograph No. 300 Vol 14, Introduction to Flight Test Engineering, 1995.

[10] R. Benjamin, et al. "Fourier could be a data scientist: From graph Fourier transform to signal processing on graphs." *Comptes Rendus. Physique*, 2019, pp. 474-488.

[11] G. Toh and J. Park, "Review of Vibration-Based Structural Health Monitoring Using Deep Learning," *Applied Sciences*, vol. 10, no. 5, p. 1680, Mar. 2020, doi: 10.3390/app10051680.

[12] D. Łuczak "Mechanical vibrations analysis in direct drive using CWT with complex Morlet wavelet." *Power Electronics and Drives*, vol.8, no.1, 2023, pp.65-73.

[13] N. K. Govindaraju, B. Lloyd, Y. Dotsenko, B. Smith and J. Manferdelli, "High performance discrete Fourier transforms on graphics processors," *SC '08: Proceedings of the 2008 ACM/IEEE Conference on Supercomputing*, Austin, TX, USA, 2008, pp. 1-12, doi: 10.1109/SC.2008.5213922.

[14] L. Muślewski, M. Pająk, A. Grządziela, and J. Musiał, "Analysis of vibration time histories in the time domain for propulsion systems of minesweepers," *Journal of Vibroengineering*, Vol. 17, No. 3, pp. 1309–1316, May 2015.

[15] T. Yang, *Telemetry Theory and Methods in Flight Test*. China: Springer, 2021, pp. 1-475, doi: 10.1007/978-981-33-4737-3.

[16] P. Quinn, "Optimizing PCM Bandwidth Usage in Flight Test by Real-Time Data Analysis During Flight," *International Telemetering Conference Proceedings,* 2022, pp. 1-6, doi: 10.5162/ettc2022/7.3.

[17] A. Devasa, M. Chorro and B. Vidal," Comparison of computing efficiency among FFT, CZT and Zoom FFT in THz-TDS" *ArXiv*. 2021, pp. 1-10, doi: /abs/2108.03948.

[18] O. ÇUlha and Y. Tanik, "Low Complexity Keystone Transform and Radon Fourier Transform Utilizing Chirp-Z Transform," *in IEEE Access*, vol. 8, pp. 105535-105541, 2020, doi: 10.1109/ACCESS.2020.3000998.

[19] Y. Wang, L. Zheng, Y. Gao and S. Li, "Vibration Signal Extraction Based on FFT and Least Square Method," in

IEEE Access, vol. 8, pp. 224092-224107, 2020, doi: 10.1109/ACCESS.2020.3044149.

[20] M. Nie, and W. Ling, "Review of condition monitoring and fault diagnosis technologies for wind turbine gearbox," *Procedia Cirp*, vol. 11, 2012, pp. 287-290, doi: 10.1016/j.procir.2013.07.018.

[21] R. Wald, T. Khoshgoftaar and J. C. Sloan, "Fourier transforms for vibration analysis: A review and case study," *2011 IEEE International Conference on Information Reuse & Integration*, Las Vegas, NV, USA, 2011, pp. 366-371, doi: 10.1109/IRI.2011.6009575.

[22] B. N. Mohapatra and R. K. Mohapatra, "FFT and sparse FFT techniques and applications," 2017 *Fourteenth International Conference on Wireless and Optical Communications Networks (WOCN),* Mumbai, India, 2017, pp. 1-5, doi: 10.1109/WOCN.2017.8065859.

[23] A. D. Das and K. K. Mahapatra, "Real-Time Implementation of Fast Fourier Transform (FFT) and Finding the Power Spectrum Using LabVIEW and Compact RIO," *2013 International Conference on Communication Systems and Network Technologies*, Gwalior, India, 2013, pp. 169-173, doi: 10.1109/CSNT.2013.45.

[24] L. Wenqiu and C. Peng, "GHz wideband real-time FFT algorithm based on FPGA," *2013 International Conference on Information and Network Security (ICINS 2013),* Beijing, 2013, pp. 1-5, doi: 10.1049/cp.2013.2475.

[25] P. Pariyal, D. Koyani, D. Gandhi, S. Yadav, D. Shah, and A. Adesara, "Comparison based Analysis of Different FFT Architectures," *International Journal of Image, Graphics and Signal Processing*, vol. 8, no. 6, 2016, pp. 41-47, 2016, doi: 10.5815/ijigsp.2016.06.05.

[26] L. Zengqiang, et al. "Application of FFT interpolation correction algorithm based on window function in power harmonic analysis." *IOP Conference Series: Earth and Environmental Science*, vol. 252, no. 3, pp. 1-8, 2019, doi: doi:10.1088/1755-1315/252/3/032184.

[27] D. Jwo, I. Wu and Y. Chang, "Windowing Design and Performance Assessment for Mitigation of Spectrum Leakage," *International Symposium on Global Navigation Satellite System 2018*, vol. 94, pp. 1-8, 2019, doi: 10.1051/e3sconf/20199403001.

[28] "Windows and Spectral Leakage," community.sw.siemens.com. https://community.sw.siemens.com/s/article/windows-and-spectral-leakage (accessed Sep. 5, 2023).

[29] D. Jwo, W. Chang and I. Wu, "Windowing techniques, the welch method for improvement of power spectrum estimation," *Computers, Materials & Continua*, 2021, pp. 3983–4003.

[30] P. Podder, et al. "Comparative performance analysis of hamming, hanning and blackman window." *International Journal of Computer Applications,* vol. 96, no. 18, pp. 1-7, 2014, doi: 10.5120/16891-6927.

[31] Y. Xiong, et al. "Accurate and robust displacement measurement for FMCW radar vibration monitoring," *IEEE Sensors Journal*, vol. 18, no. 3, pp. 1131-1139, 1 Feb.1, 2018, doi: 10.1109/JSEN.2017.2778294.

[32] J. Rabi, T. Balusamy, and R. Raj Jawahar. "Analysis of vibration signal responses on pre induced tunnel defects in friction stir welding using wavelet transform and empirical mode decomposition," *Defence Technology*, volume 15, No 6, pp. 885-896, 2019, doi: 10.1016/j.dt.2019.05.014.

[33] A.D. Poularikas, *Transforms and Applications Handbook.* Arkansas: CRC Press, 2010.

[34] J. Wang, Y. Peng and W. Qiao, "Current-Aided Order Tracking of Vibration Signals for Bearing Fault Diagnosis of Direct-Drive Wind Turbines," *in IEEE Transactions on Industrial Electronics*, vol. 63, no. 10, pp. 6336-6346, Oct. 2016, doi: 10.1109/TIE.2016.2571258.

[35] B. Xu, T. Han, Z. Zhang, X. Liu and M. Ju, "Research on Sub-Nyquist Rate Sampling Method Based on Sparse Fourier Transform Theory," *2021 IEEE 4th International Conference on Electronics Technology (ICET)*, Chengdu, China, 2021, pp. 742-747, doi: 10.1109/ICET51757.2021.9450919.

[36] D. Vazhenina and K. Markov, "End-to-End Noisy Speech Recognition Using Fourier and Hilbert Spectrum Features," *Electronics,* vol. 9, no. 7, pp. 1-18, Jul. 2020, doi: 10.3390/electronics9071157.

[37] H. Jeon, Y. Jung, S. Lee, and Y. Jung, "Area-Efficient Short-Time Fourier Transform Processor for Time–Frequency Analysis of Non-Stationary Signals," *Applied Sciences*, 2020, vol. 10, no. 20, pp. 1-10, Oct. 2020, doi: 10.3390/app10207208.

[38] O. Arslan and M. Karhan, "Effect of Hilbert-Huang transform on classification of PCG signals using machine learning," *Journal of King Saud University - Computer and Information Sciences*, Volume 34, No 10, pp. 9915-9925, 2022, doi: 10.1016/j.jksuci.2021.12.019.

[39] M. Rhif, A. Ben Abbes, I. Farah, B. Martínez, and Y. Sang, "Wavelet Transform Application for/in Non-Stationary Time-Series Analysis: A Review," *Applied Sciences*, vol. 9, no. 7, pp. 1-22, Mar. 2019, doi: 10.3390/app9071345.

[40] M. Mishra, "Power quality disturbance detection and classification using signal processing and soft computing techniques: A comprehensive review," *Int Trans Electr Energ Syst*, vol. 29, no. 8, pp. 1-41, 2019, doi: 10.1002/2050-7038.12008.

[41] Y. Hu, Z. Wang, X. Wang, et al. "Efficient full-path optical calculation of scalar and vector diffraction using the Bluestein method". Light: Science & Applications 9, vol. 9, no. 1, pp. 1-11, 2020, doi: 10.1038/s41377-020-00362-z.

[42] S. Scherr, et al. "An efficient frequency and phase estimation algorithm with CRB performance for FMCW radar applications." *IEEE Transactions on Instrumentation and Measurement*, vol. 64, no. 7, pp. 1868-1875, July 2015, doi: 10.1109/TIM.2014.2381354.

[43] M. Shuohan, M. A. Qishuang, and L. Xinbo. "Applications of chirp z transform and multiple modulation zoom spectrum to pulse phase thermography inspection," *NDT & E International*, vol. 54, pp. 1-8, 2013, doi: 10.1016/j.ndteint.2012.11.006.

[44] K. Wang, L. Wang, B. Yan and H. Wen, "Efficient Frequency Estimation Algorithm Based on Chirp-Z Transform," *in IEEE Transactions on Signal Processing*, vol. 70, pp. 5724-5737, 2022, doi: 10.1109/TSP.2022.3224648.

[45] P. A. Milder, F. Franchetti, J. C. Hoe and M. Püschel, "Hardware implementation of the discrete fourier transform with non-power-of-two problem size," *2010 IEEE International Conference on Acoustics, Speech and Signal Processing*, Dallas, TX, USA, 2010, pp. 1546-1549, doi: 10.1109/ICASSP.2010.5495517.

[46] G. Plonka, D. Potts, G. Steifdl and M. Tasche. *Numerical Fourier Analysis*. USA: Birkhauser, 2018, pp. 1-615.

[47] I. Kubiak and A. Przybysz, "Fourier and Chirp-Z Transforms in the Estimation Values Process of Horizontal and Vertical Synchronization Frequencies of Graphic Displays," *Applied Sciences*, 2022, vol. 12, no. 10, pp. 1-18, May 2022, doi: 10.3390/app12105281.

[48] T. T. Wang, "The segmented chirp Z-transform and its application in spectrum analysis," *in IEEE Transactions on Instrumentation and Measurement*, vol. 39, no. 2, pp. 318-323, April 1990, doi: 10.1109/19.52508.

[49] S. Murugan and K. Jayakumar, "A DSP based real-time 3D FFT system for analysis of dynamic parameters," *2014 IEEE International Conference on Advanced Communications, Control and Computing Technologies*, Ramanathapuram, India, 2014, pp. 1489-1492, doi: 10.1109/ICACCCT.2014.7019351.

[50] Z. D. Tsai, H. S. Wang, J. C. Chang, and J. R. Chen, "Development of an On-line System for Vibration

Measurement and Tracing" *Particle Accelerator Conference (PAC)*, Canada, 2009, pp. 3660–3662.
[51] G. Wang, X. Wang, and C. Zhao, "An Iterative Hybrid Harmonics Detection Method Based on Discrete Wavelet Transform and Bartlett–Hann Window," *Applied Sciences*, vol. 10, no. 11, pp. 1-16, Jun. 2020, doi: 10.3390/app10113922.
[52] L. Sevgi, "Numerical Fourier Transforms: DFT and FFT," in *IEEE Antennas and Propagation Magazine*, vol. 49, no. 3, pp. 238-243, June 2007, doi: 10.1109/MAP.2007.4293982.
[53] R. Puche-Panadero et al., "New Method for Spectral Leakage Reduction in the FFT of Stator Currents: Application to the Diagnosis of Bar Breakages in Cage Motors Working at Very Low Slip," in *IEEE Transactions on Instrumentation and Measurement*, vol. 70, pp. 1-11, 2021, Art no. 3511111, doi: 10.1109/TIM.2021.3056741.
[54] J. Semmlow, *Circuits, Signals, and Systems for Bioengineers*. New Brunswick: ELSEVIER, 2005.
[55] "TEC-NOT-019," curtisswrightds.com. https://www.curtisswrightds.com/resources/tec-not-019-introduction-digital-filtering (accessed Oct. 15, 2023).
[56] "KAD/ADC/111," curtisswrightds.com. https://www.curtisswrightds.com/products/flight-test/data-acquisition/acrakam500/analog/kadadc111 (accessed Oct. 22, 2023).
[57] C. Moler, and L. Jack, "A history of MATLAB." *Proceedings of the ACM on Programming Languages*, vol. 7, no. OOPSLA2, pp. 1-67, 2020, doi: 10.1145/3622797.
[58] "Model 339B31 Accelerometer," pcb.com. https://www.pcb.com/products?m=339b31 (accessed Nov. 2, 2023).
[59] S. Chen, and X. Li, "A hybrid GPU/CPU FFT library for large FFT problems," *2013 IEEE 32nd International Performance Computing and Communications Conference (IPCCC),* San Diego, CA, USA, 2013, pp. 1-10, doi: 10.1109/PCCC.2013.6742796.
[60] H.C. Lin, and Y. Ye, "Reviews of bearing vibration measurement using fast Fourier transform and enhanced fast Fourier transform algorithms," *Advances in Mechanical Engineering*, vol. 11, no. 1, pp. 1-12, 2019, doi: 10.1177/1687814018816751.
[61] W. Tian, J. Yu, X. Ma, and J. Li, "Power System Harmonic Detection Based on Bartlett-Hann Windowed FFT Interpolation," *2012 Asia-Pacific Power and Energy Engineering Conference*, Shanghai, China, 2012, pp. 1-3, doi: 10.1109/APPEEC.2012.6307426.
[62] D. Hou, H. Qi, H. Luo, C. Wang, and J. Yang, "Comparative study on the use of acoustic emission and vibration analyses for the bearing fault diagnosis of high-speed trains," *Structural Health Monitoring,* vol. 21, no.4, pp. 1-23, 2021, doi: 10.1177/1475921721103602.